

*Full Length Research Paper*

# Omnidirectional High Reflectors using 1-D Photonic Crystals

Pandey J. P.

Department of Physics, Maharani Lal Kunwari P.G. College (M L K P G), Balrampur (UP) - 271201, India.

Received 8 April, 2017; Accepted 20 June, 2017

**Much interest has been paid to omnidirectional dielectric mirrors based on the 1-D dielectric multilayers because these are better than metal mirrors owing to their low optical loss, high reflectivity and high mechanical robustness. In these applications, the required position and width of the reflection band can be obtained by adjusting the layer thickness and refractive indices of the constituent materials. Here, the omnidirectional reflection characteristics of a 1-D PC formed by  $\text{TiO}_2/\text{SiO}_2$  multi-quantum wells (MQW) are investigated in the visible region. It is demonstrated that the omnidirectional high reflector, formed by the proper line-up of four  $\text{TiO}_2/\text{SiO}_2$  MQWs, covers the visible band approximately when the number of periodic layers of each quantum well reaches 12. This study can provide guidance in the design of an omnidirectional high reflector in the visible band.**

**Key words:** Omnidirectional reflector, photonic crystals, multi-quantum wells.

## INTRODUCTION

In recent years, omnidirectional reflection i.e. nearly 100% reflectivity at all incident angles for both transverse electric (TE) and transverse magnetic (TM) modes by a periodic 1-D medium has much attention from various research groups of the field. Fink et al. (1998) and Winn et al. (1998) firstly designed the omnidirectional reflection in 1-D photonic crystal and demonstrated it over a wavelength range from 10 to 15  $\mu\text{m}$ . A lattice consisting of 19 layers of  $\text{Na}_3\text{AlF}_6$  and  $\text{ZnSe}$  was fabricated by Chigrin et al. (1999a; b) and they observed the omnidirectional band gap in the frequency range 604.3 to 638.4 nm. Lee and Yao (2003) investigated different structures theoretically and experimentally for a realistic fabrication of 1-D photonic bandgap materials, exhibiting

omnidirectional band gaps (OBGs) in 2003.

The application of one-dimensional photonic crystals in various optoelectronic devices is found to be cheap and effective because their fabrication is relatively easy. The 1-D PCs can be fabricated by using different deposition techniques such as electron beam evaporation, sol-gel method, holography and r.f.-sputtering etc. The different materials used to fabricate 1-D PCs for OBGs in various frequency ranges are tellurium/polyethylene for infrared (Fink et al., 1998),  $\text{TiO}_2/\text{SiO}_2$  (Valligatla et al., 2012) for near infrared (NIR) and  $\text{TiO}_2/\text{SiO}_2$  (Lin et al., 2005) for visible light.  $\text{TiO}_2$  and  $\text{SiO}_2$  are non-absorbing and non-dispersive high and low index dielectric oxide materials having good refractive index contrast, and are used for

E-mail: [jpandeymlk@gmail.com](mailto:jpandeymlk@gmail.com). Tel: +919450517226.

Author(s) agree that this article remain permanently open access under the terms of the [Creative Commons Attribution License 4.0 International License](https://creativecommons.org/licenses/by/4.0/)

visible range.  $\text{TiO}_2/\text{SiO}_2$  multilayer is investigated for very high reflectivity band gaps in the visible NIR region and omnidirectional reflectivity in the visible region with nearly 100% reflection (Jena et al., 2016).

The photonic band gap (PBG) of photonic crystals (PCs) can be enlarged by arranging the PCs with an asymmetric topology structure (Giden and Kurt, 2012) when choosing dielectric materials as a constituent (Zhang et al., 2013b) and introducing the metamaterials into PCs (El-Naggar, 2013). In these methods, the first one is a better choice to enlarge the PBGs. Recently the PBGs are enhanced in 1-D plasma photonic crystals (PPCs) with Fibonacci or Thue–Morse quasi-periodic structure (Zhang et al., 2013c; 2013d) heterostructure, staggered and cascaded structure (Pandey, 2017). The plasma photonic crystals with fractal structures can also enlarge the bandwidths of PBGs. Segev et al. (2012) reported that the fractal structure has a wide range of applications in optics. A lot of fractal topology structures such as the Cantor, Sierpinski gasket, Menger sponge and Koch fractal structures are found in the nature. The subwavelength or compacted devices can be constructed by introducing the fractal structures (Zhang and Chen, 2017; Zhang and Liu, 2016a).

Hojo and colleagues introduced firstly the plasma into the photonic crystals to realize the plasma photonic band gaps in 2004. The external magnetic field, electron-temperature and plasma density can affect the properties of plasma easily. The PPCs show an enlargement and a tunability of the PBG (Zhang et al., 2009; Zhang and Liu, 2016b) as compared to the conventional dielectric PCs. Various research groups worldwide have studied both theoretically (Prasad et al., 2011; Wu et al., 2010; Zhang et al., 2013a) and experimentally (Fan et al., 2010) during the past ten years about it. Also, the enhancements of the PBGs can be done by using superconductor-dielectric photonic crystal which may be used as broad band reflector and omnidirectional reflector at low temperature below to the critical temperature (Pandey et al., 2016a; b).

Also, 1-D photonic crystal made of Si was theoretically studied for high frequency range of omnidirectional reflection by Singh et al. (Singh et al., 2006; Singh et al., 2007) and Thapa et al. (2006) who investigated 1-D omnidirectional high reflector for infrared wavelengths. They demonstrated that, two Si-based photonic crystals increase the frequency range of OBG by overlapping. Various researches demonstrated a relatively narrow OBG for the visible region and also the lack of suitable materials for omnidirectional high reflectors in visible and near-infrared bands. Two types of reflectors made of metals and multilayers of dielectric are generally found. The reflectivity of metallic reflectors is found to be good over a large frequency range for arbitrary angles of incidence but much power is attenuated due to absorption at visible, optical, or higher frequencies whereas multilayer dielectric reflectors show high reflectivity for p

articular frequency ranges and are very low lossy.

The proper choice of high and low refractive index materials (Guan et al., 2011; Kumar et al., 2011; Liu et al., 2015) can broaden the OBG and PBG but there are few materials with high index of refraction in the visible region. So, it is difficult to broaden the OBG and PBG, in the visible spectrum. It is found that the introduction of defects and multi-quantum wells (MQWs) (Liu et al., 2015) are very effective for the broadening of the band gap. The desired range of omnidirectional band gap (OBG) was obtained by Wang et al. (2002) from multiple photonic heterostructures formed by more than one-dimensional PCs. The high reflectivity and omnidirectional reflection of multilayer dielectric reflectors can be obtained by using photonic quantum wells (Fink et al., 1998; Guan et al., 2011; Liu et al., 2015).

In this communication, quantum wells are introduced for obtaining the large frequency range of OBG in the visible spectrum.  $\text{TiO}_2$  and  $\text{SiO}_2$  are taken as two kinds of optical materials having good refractive index contrast and less absorption in the visible region.

## MATERIAL AND METHODS

In the Transfer Matrix Method (Born and Wolf 1980; Yeh, 1988), the Maxwell's equations are arranged in the k-space and a mesh is formed. It performs layer by layer calculation of multilayers having finite thickness of photonic crystals. The photonic bandgap structures with defects can be studied by considering a super-cell. The band structures, reflectivity and transmission coefficients can be found by this method easily. Many researchers are using this method because the theoretical data obtained from it is in excellent agreement with experimental data. The limitations of this method are the memory storage and also there is a problem to describe the geometry different from the cubic geometry.

Consider a periodic multilayered structure in which electromagnetic wave is propagating. This multilayered structure consists of alternate layers of materials with different refractive indices. The schematic diagram of a multilayered 1-D PC structure is shown in Figure 1, where  $n_i$  is the index of refraction of the media of incidence and  $n_s$  is the index of refraction of substrate. The refractive index profile of the multilayer is given below,

$$n(x) = \begin{cases} n_1 & 0 < x < d_1 \\ n_2 & d_1 < x < d \end{cases} \quad \text{with } n(x) = n(x+d) \quad (1)$$

where  $n_1$  and  $n_2$  are the refractive indices of two layers and  $d_1$  and  $d_2$  are their respective thicknesses.  $d = d_1 + d_2$  is the period of a structure.

Using the transfer matrix method (Born and Wolf 1980; Yeh, 1988), the photonic spectra of this periodic structure are derived. The equation of the electric field is written with the help of Maxwell's equation. The electric field within layer with index  $n_1$  is,

$$\vec{E}(x) = A_1 e^{ik_1 x} + B_1 e^{-ik_1 x} \quad (2)$$

and,

$$\vec{E}(x) = C_1 e^{ik_2 x (x-d_1)} + D_1 e^{-ik_2 x (x-d_1)} \quad (3)$$

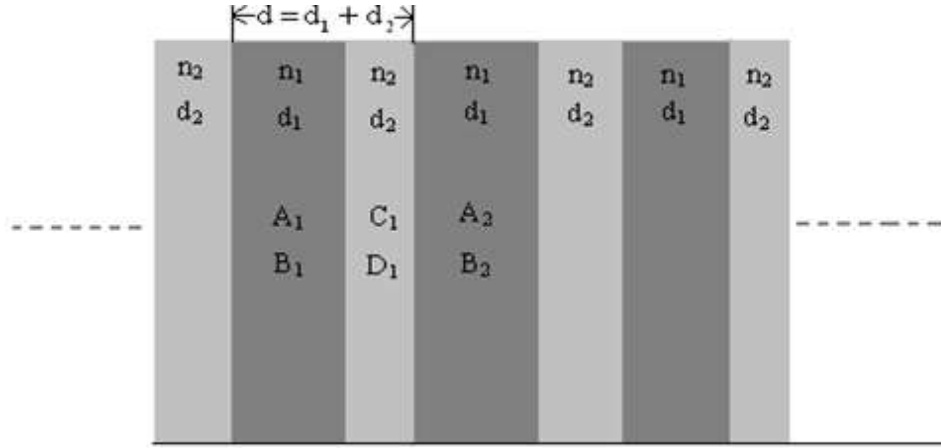


**Figure 1.** Schematic diagram of a multilayered dielectric photonic crystal structure.

for the layer with index  $n_2$ . The parameter  $k_{1x}$  and  $k_{2x}$  are called wave number, and the definition is given by the equation;

$$k_{1x} = \frac{\omega}{c} n_1 \cos \theta_1 \quad \text{and} \quad k_{2x} = \frac{\omega}{c} n_2 \cos \theta_2 \quad (4)$$

where,  $\theta_1$  and  $\theta_2$  are the ray angles in the two mediums, respectively.

At the interface between layers ( $x = d_1$ ), the solution and its derivative should be continuous. This gives a relation between plane waves amplitude:

$$\begin{pmatrix} C_1 \\ D_1 \end{pmatrix} = M_{12} \begin{pmatrix} A_1 \\ B_1 \end{pmatrix} \quad (5)$$

with

$$M_{12} = \begin{pmatrix} \frac{1}{2} \left( 1 + \frac{k_{1x}}{k_{2x}} \right) e^{ik_{1x}d_1} & \frac{1}{2} \left( 1 - \frac{k_{1x}}{k_{2x}} \right) e^{-ik_{1x}d_1} \\ \frac{1}{2} \left( 1 - \frac{k_{1x}}{k_{2x}} \right) e^{ik_{1x}d_1} & \frac{1}{2} \left( 1 + \frac{k_{1x}}{k_{2x}} \right) e^{-ik_{1x}d_1} \end{pmatrix} \quad (6)$$

and, also at  $x = d$ , the continuity of the plane waves at the interface is between layers with indices  $n_2$  and  $n_1$  and its derivative gives

$$\begin{pmatrix} A_2 \\ B_2 \end{pmatrix} = M_{21} \begin{pmatrix} C_1 \\ D_1 \end{pmatrix} \quad (7)$$

where the matrix  $M_{21}$  is the same as (6) interchanging the indices. From the two matrix equations (5) and (7), we have;

$$\begin{pmatrix} A_2 \\ B_2 \end{pmatrix} = M_{21} M_{12} \begin{pmatrix} A_1 \\ B_1 \end{pmatrix} \quad \text{or} \quad \begin{pmatrix} A_2 \\ B_2 \end{pmatrix} = M_{i,j} \begin{pmatrix} A_1 \\ B_1 \end{pmatrix} \quad (8)$$

where  $M_{i,j} = M_{21} M_{12}$ . The matrix element of the matrix  $M_{i,j}$  is given

by,

$$M_{11} = e^{ik_{1x}d_1} \left[ \cos(k_{2x}d_2) + \frac{1}{2}i \left( \gamma + \frac{1}{\gamma} \right) \sin(k_{2x}d_2) \right] \quad M_{12} = e^{-ik_{1x}d_1} \left[ +\frac{1}{2}i \left( \frac{1}{\gamma} - \gamma \right) \sin(k_{2x}d_2) \right]$$

$$M_{2,1} = \overline{M}_{1,2}, \quad M_{2,2} = \overline{M}_{1,1},$$

where  $k_{jx} = \frac{\omega}{c} n_j \cos \theta_j$  and  $\gamma = \frac{k_{1x}}{k_{2x}}$  for TE mode, and

$$\gamma = \frac{k_{1x} \times n_2^2}{k_{2x} \times n_1^2} \quad \text{for TM mode.}$$

The matrix  $M_{i,j}$  is called the transfer matrix of one unit of a periodic lattice. The matrix  $M_{i,j}$  depends on the frequency  $\omega$ , and it is unimodular (it is a square matrix with determinant equal to unity). Hence, for each  $\omega$ , the matrix  $M_{i,j}$  defines a unique mapping for amplitudes of the plane waves in layer  $n_1$  into the amplitude of the next layer with index  $n_2$ .

The coefficients of right and left hand side propagating waves in both sides of multilayer structures of  $N$  periods are calculated by multiplying transfer matrices of each cell as given below,

$$\begin{pmatrix} A_0 \\ B_0 \end{pmatrix} = M_1 M_2 \dots M_N \begin{pmatrix} A_N \\ B_N \end{pmatrix} \quad (9)$$

The coefficient of reflection can be found as

$$r_N = \begin{pmatrix} A_0 \\ B_0 \end{pmatrix}_{B_N=0} \quad (10)$$

The reflectance is calculated as,

$$R_N = |r_N|^2 \quad (11)$$

The phenomenon of propagation of electromagnetic waves through multilayered periodic structure is similar to the motion of electrons in

solid crystals. So, the electromagnetic waves can be compared by the Bloch waves and the following dispersion relation is satisfied (Yeh, 1988).

$$K(\beta, \omega) = \frac{1}{h} \cos^{-1} \left[ \frac{M_{11} + M_{22}}{2} \right] \tag{12}$$

where  $K(\beta, \omega)$  is the Bloch wave number.

When  $\left[ \frac{M_{11} + M_{22}}{2} \right] < 1$ ,  $K(\beta, \omega)$  is the real number, the

electromagnetic wave can transmit through the multilayer.

$\left[ \frac{M_{11} + M_{22}}{2} \right] > 1$ ,  $K(\beta, \omega)$  is an imaginary number, in this

condition, wave cannot transmit through 1-D PC and is totally reflected. This corresponds to the band gap of the structure. When

$\left[ \frac{M_{11} + M_{22}}{2} \right] = 1$  edges of the band gap of the photonic

crystal is found.

To understand the condition for the existence of omnidirectional reflection in 1D-PC, the Snell's law is given as,

$n_i \sin \theta_i = n_H \sin \theta_H$  and  $n_H \sin \theta_H = n_L \sin \theta_L$  where  $n_H$  and  $n_L$  are the high and low refractive indices of media,  $n_i$  is the index of refraction of medium of incidence. The internal Brewster

angle  $\theta_B = \tan^{-1} \frac{n_L}{n_H}$  is greater than maximal refracted angle,

the incident wave will be totally reflected for all angles of incidence.

So, the necessary condition of the omnidirectional is  $\theta_B > \theta_H^{Max}$ ,

where  $\theta_H^{Max} = \sin^{-1} \left( \frac{n_i}{n_H} \right)$  is the maximum refractive angle of

the light in high index medium. The difference between lower band edge at the normal incidence and the upper band edge at the perpendicular incidence is the OBG for both TE and TM polarizations.

## RESULTS AND DISCUSSION

Here, the 1-D photonic crystal is considered as a multilayer periodic structure composed of multi-quantum wells (MQWs). It has  $TiO_2$  as a high refractive index and  $SiO_2$  as a low refractive index material. The structures  $(AB)_m$ ,  $(CD)_n$ ,  $(EF)_l$  and  $(GH)_s$  composed of  $TiO_2$  and  $SiO_2$  are considered for the study.

A, C, E and G represent  $TiO_2$ ; B, D, F and H represent  $SiO_2$ . m, n, l and s denote the number of periodic layers of structure. The quantum well unit cell constant is represented as  $d_i$ , and  $d_1 = d_A + d_B$ ,  $d_2 = d_C + d_D$ ,  $d_3 = d_E + d_F$ ,  $d_4 = d_G + d_H$ . The PBG and OBG of the photonic quantum well of  $TiO_2/SiO_2$  can be investigated by the transfer matrix method. The thicknesses  $d_i$  are taken according to the quarter wave stack arrangement as  $d_i =$

$\lambda_0/4.n_i$ . The central wavelengths are taken as 800, 680, 560 and 440 nm for the structures  $(AB)_m$ ,  $(CD)_n$ ,  $(EF)_l$  and  $(GH)_s$  respectively. The thicknesses values are  $d_A=86.96$ ,  $d_B=133.33$ ,  $d_C=73.91$ ,  $d_D=113.33$ ,  $d_E=60.87$ ,  $d_F=93.33$ ,  $d_G=47.83$  and  $d_H=73.33$ .

Figure 2(a) to 6(a) represents the 100% reflection regions of Transverse electric (TE) and Transverse magnetic (TM) modes. If the angle of incidence is  $0^\circ$ , the PBGs are completely overlapped in both TE and TM modes. When the angle of incidence is  $0^\circ$  to  $30^\circ$ , the width of the band gap and the reflectivity rate is stable for two polarized modes. But when the angle of incidence is between  $30^\circ$  and  $85^\circ$ , band gap decreases and the gap width of the TM mode becomes narrower. Therefore, the reflectance spectra of the combined structure of the four quantum wells were theoretically investigated.

Firstly, a 1-D PC  $(AB)_m$  is considered which consists of 12 periodic layers of  $TiO_2$  and  $SiO_2$ . Their refractive indices are 2.3 and 1.5, respectively. This 1D-PC structure is on a substrate of glass having refractive index  $n_s = 1.5$  and medium of incidence is air  $n_i = 1.0$ . The thickness of the layers is chosen in accordance with the quarter wave arrangement, where  $d_H$  and  $d_L$  are the thicknesses of the  $TiO_2$  and  $SiO_2$  layers. According to this condition,  $d_H = 86.96$  nm and  $d_L = 133.33$  nm. For this,

photonic crystal structure,  $\theta_H^{Max} = \sin^{-1} \left( \frac{n_i}{n_H} \right) = 25.096$

degree and  $\theta_B = \tan^{-1} \left( \frac{n_L}{n_H} \right) = 31.914$  degree.

Since  $\theta_B > \theta_H^{Max}$ , the condition of omnidirectional reflection is satisfied. The reflectance of TE polarizations at  $0^\circ$ ,  $45^\circ$  and  $85^\circ$  angles and TM polarizations at  $0^\circ$ ,  $45^\circ$  and  $70^\circ$  angles are represented in Figure 2(a). Figure 2(b) shows the conventional photonic band structure which is obtained by the projection of reflectivity values  $R \approx 1$  from Figure 2(a). The grey and white regions of Figure 2(b) represent the forbidden and allowed bands, respectively. The values of frequency regions having nearly 100% reflectivity are shown in the Table 1 and the omnidirectional reflection range (ODR) is represented by the black area between two horizontal lines in Figure 2. In this structure, both the polarizations (TE and TM) possess omnidirectional reflection when angle of incidence is below  $70^\circ$ . ODR is found from  $\lambda_H = 718$  to  $\lambda_L = 710$  nm, with bandwidth  $\Delta\lambda = (\lambda_H - \lambda_L) = 8$  nm. ODR is not present for incident angles greater than  $75^\circ$ .

Similarly, the reflectance spectra and photonic band structure of the periodic 1-D PCs  $(CD)_n$ ,  $(EF)_l$ , and  $(MN)_s$  are shown in Figures 3 to 5 and the corresponding data are shown in the Tables 2 to 5. The spectra and band structure of four combined multi-quantum wells (MQWs)

**Table 1.** Region of total reflection and bandgap width for  $(AB)_m$  1-D PC having 12 layers.

Incident angle, $\theta_i$ (degree)	TE polarization		TM polarization (98%)	
	Reflection range (nm)	Gap width (nm)	Reflection range (nm)	Gap width (nm)
0	710-920	210	710-920	210
30	673-896	223	689-869	180
50	622-862	240	659-799	140
70	573-833	260	642-718	76
85	553-825	272	-	-

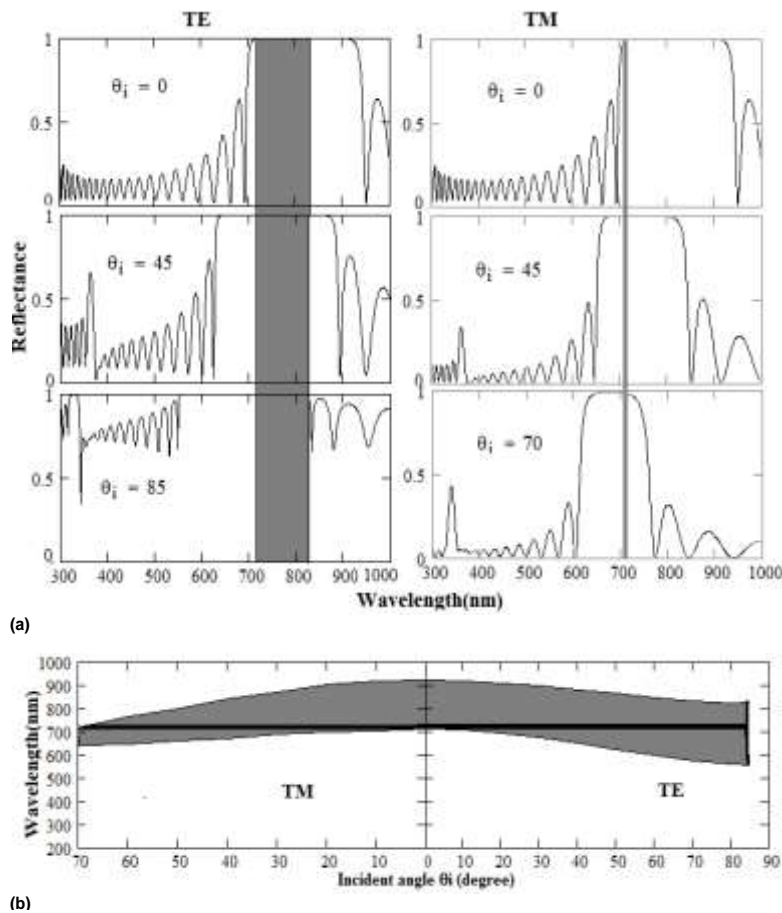


**Figure 2.** (a) Reflectance of TE and TM polarizations of twelve-pairs of  $(AB)_m$  1-D PC at various angles (b) their photonic band structure.

are shown in Figure 6{(a) to (b)}. For TE polarization, the bandgap of the four combined MQWs lies between 396 and 824 nm which covers both visible and near-infrared region. For TM polarization, the PBG lies between 396 and 726 nm. The ODR is demonstrated in the region of 396 to 726 nm when the number of periodic layers reached 12 and covers the visible region approximately. Thus, the goal of omnidirectional high reflector is achieved in the visible band.

### Conclusion

The omnidirectional reflectance spectra of the multilayered dielectric structure composed of  $TiO_2/SiO_2$  MQW is theoretically investigated by the transfer matrix method in the visible region. It is demonstrated that the omnidirectional high reflector, formed by the proper line-up of four  $TiO_2/SiO_2$  MQWs, covers the visible band approximately, when the number of periodic layers of each quantum well reaches 12.

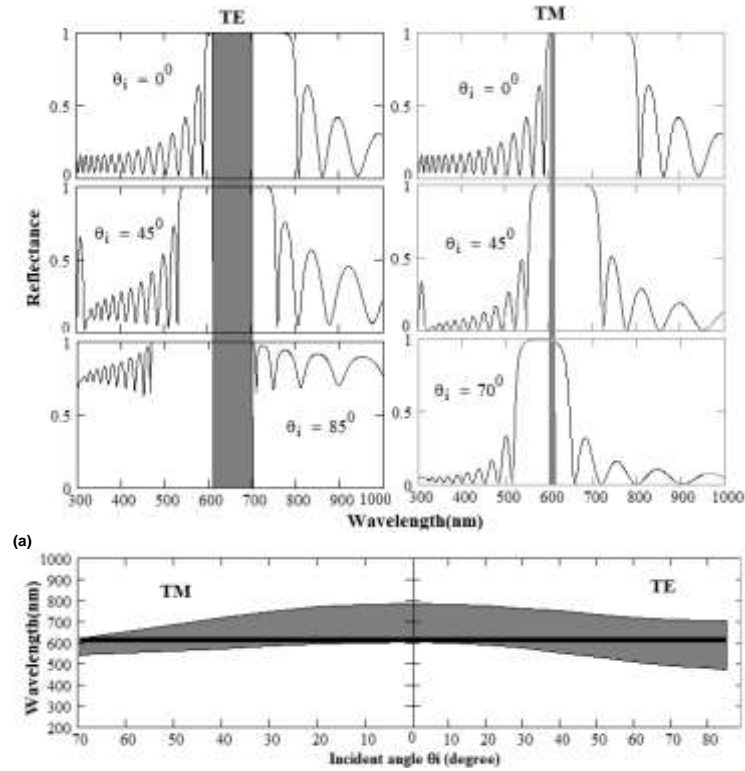


**Figure 3.** (a) Reflectance of TE and TM polarizations of twelve-pairs of  $(CD)_n$  1-D PC at various angles (b) their photonic band structure.

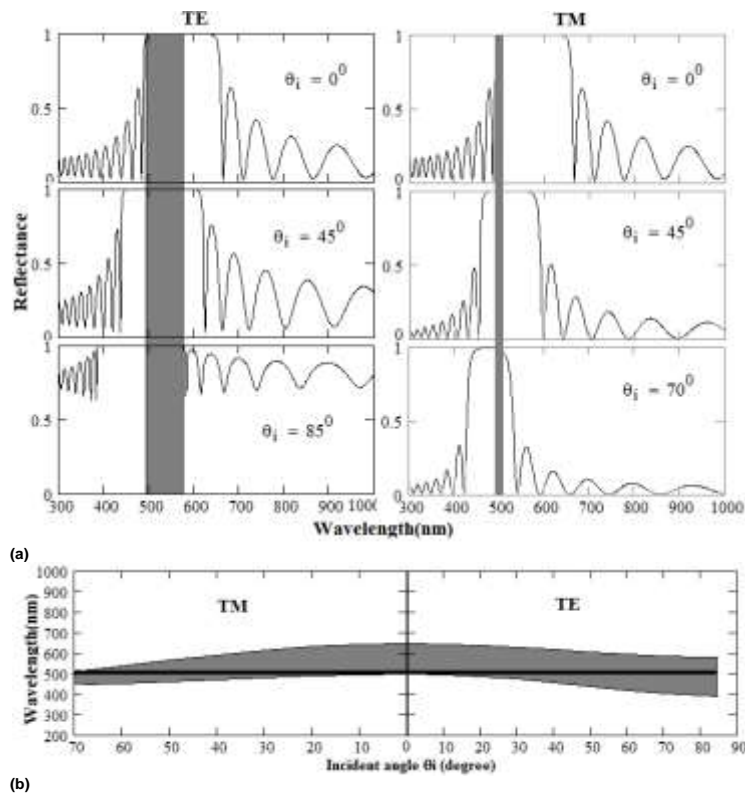


**Figure 4.** (a) Reflectance of TE and TM polarizations of twelve-pairs of (EF) 1-D PC at various angles (b) their photonic band structure.

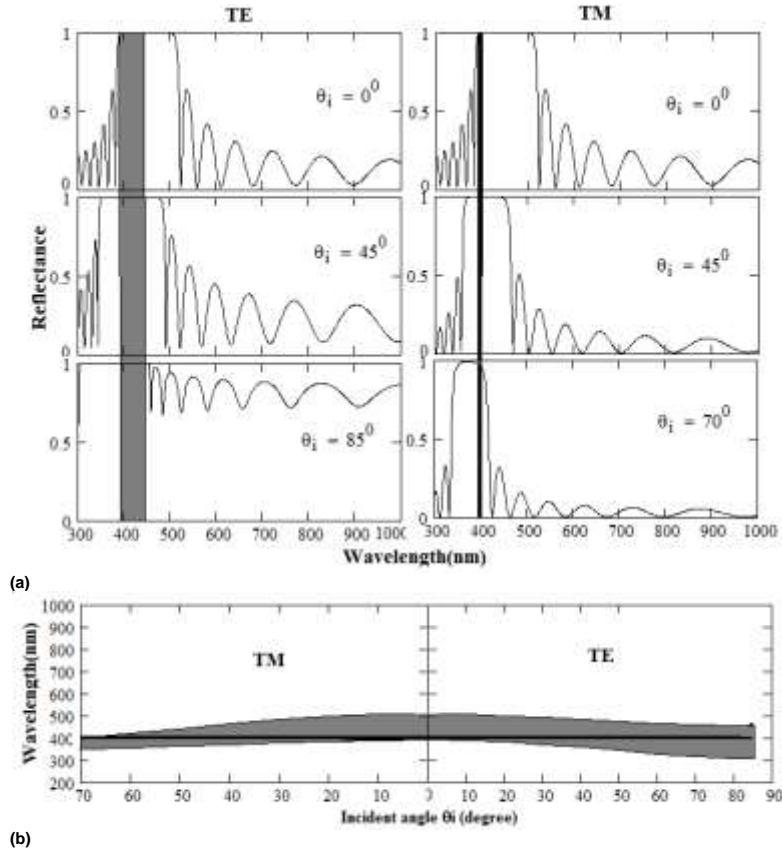


**Figure 5.** (a) Reflectance of TE and TM polarizations of twelve-pairs of  $(GH)_s$  1-D PC at various angles (b) their photonic band structure.

**Table 2.** Region of total reflection and bandgap width for  $(CD)_n$  1-D PC having 12 layers.

Incident angle, $\theta_i$ (degree)	TE polarization (99%)		TM polarization (97%)	
	Reflection range (nm)	Gap width (nm)	Reflection range (nm)	Gap width (nm)
0	603-782	179	603-782	179
30	573-761	188	582-745	163
50	529-733	204	558-682	124
70	487-708	221	541-616	75
85	470-701	231	-	-

**Table 3.** Region of total reflection and bandgap width for  $(EF)_l$  1-D PC having 12 layers.

Incident angle, $\theta_i$ (degree)	TE polarization (99%)		TM polarization (97%)	
	Reflection range (nm)	Gap width (nm)	Reflection range (nm)	Gap width (nm)
0	497-644	147	494-649	155
30	472-627	155	480-614	134
50	436-604	168	460-562	102
70	402-583	181	446-507	61
85	387-577	190	-	-

**Table 4.** Region of total reflection and bandgap width for (GH)<sub>s</sub> 1-D PC having 12 layers.

Incident angle, $\theta_i$ (degree)	TE polarization (99%)		TM polarization (97%)	
	Reflection range (nm)	Gap width (nm)	Reflection range (nm)	Gap width (nm)
0	391-506	115	391-506	115
30	371-493	122	377-482	105
50	343-474	131	362-442	80
70	316-458	142	351-399	48
85	305-454	149	-	-

**Table 5.** Region of total reflection and bandgap width for (AB)<sub>m</sub>/ (CD)<sub>n</sub>/ (EF)<sub>j</sub>/ (GH)<sub>s</sub> MQW having 12 layers.

Incident angle, $\theta_i$ (degree)	TE polarization (99%)		TM polarization (97%)	
	Reflection range (nm)	Gap width (nm)	Reflection range (nm)	Gap width (nm)
0	396-917	521	396-917	521
30	372-893	521	378-875	497
50	344-856	512	363-796	433
70	317-832	515	437-726	289
85	305-824	519	-	-

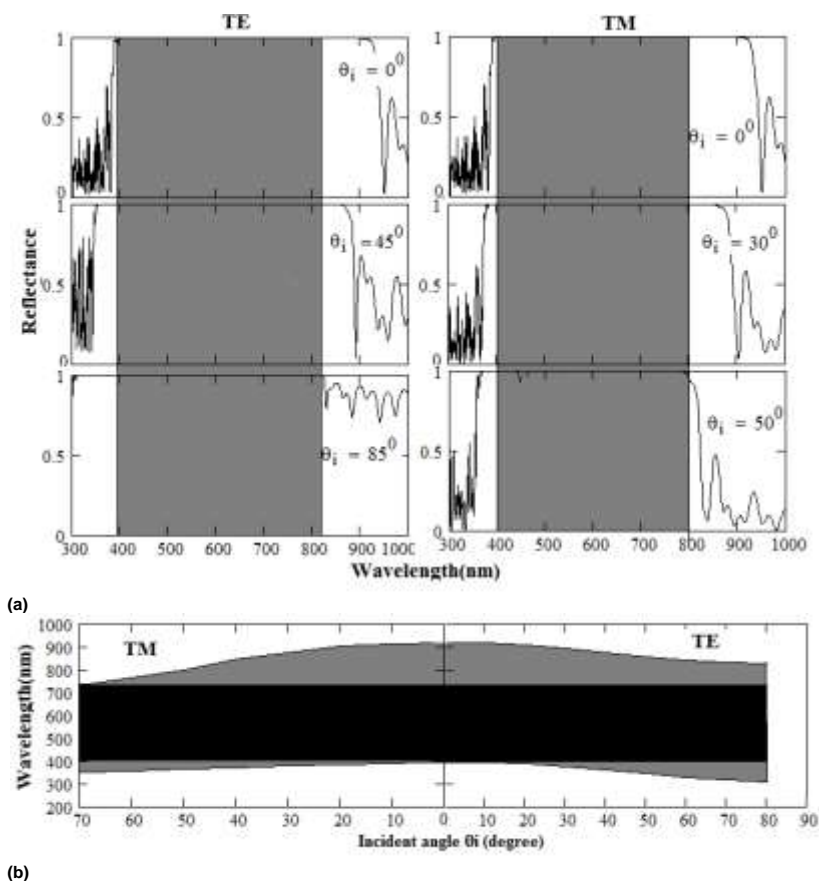


**Figure 6.** (a) Reflectance of TE and TM polarizations of twelve-pairs of (AB)<sub>m</sub>/ (CD)<sub>n</sub>/ (EF)<sub>j</sub>/ (GH)<sub>s</sub> MQWs at various angles (b) their photonic band structure.



Therefore, this work may be useful in the design of an omnidirectional high reflector in the visible spectrum as well as of the design of photo-voltaic cells.

## CONFLICT OF INTERESTS

The authors have not declared any conflict of interests.

## REFERENCES

- Born M, Wolf E (1980). *Principles of Optics* (New York: Pergamon).
- Chigrin DN, Lavrinenko AV, Yarotsky DA, Gaponenko SV (1999a). Observation of total omnidirectional reflection from a one-dimensional dielectric lattice. *Appl. Phys. A* 68:25-28.
- Chigrin DN, Lavrinenko AV, Yarotsky DA, Gaponenko SV (1999b). All-Dielectric One-Dimensional Periodic Structures for Total Omnidirectional Reflection and Partial Spontaneous Emission Control. *J. Light Wave Technol.* 17:2018-2024.
- Fan W, Zhang X, Dong L (2010). Two-dimensional plasma photonic. *Phys. Plasmas* 17:113501.
- El-Naggar SA (2013). Enlarged omnidirectional photonic gap in one dimensional ternary plasma photonic crystals that contain metamaterials. *Euro. Phys. J. D* 67:1.
- Fink Y, Winn JN, Fan S, Chen C, Michel J, Joannopoulos JD, Thomas E L (1998). A Dielectric Omnidirectional Reflector. *Science* 282:1679-1682.
- Giden IH, Kurt H (2012). Modified annular photonic crystals for enhanced band gap properties and iso-frequency contour engineering. *Appl. Opt.* 51:1287.
- Guan H, Han P, Yang Y, Li Y, Zhang X, Zhang W (2011). Omnidirectional mirror for visible light based on one-dimensional photonic crystal. *Chin. Opt. Lett.* 9(7):071603.
- Jena S, Tokas RB, Sarkar P, Misal JS, Haque SM, Rao KD, Thakur S, Sahoo NK (2016). Omnidirectional photonic band gap in magnetron sputtered TiO<sub>2</sub>/SiO<sub>2</sub> one dimensional photonic crystal. *Thin Solid Films.* Jan 29; 599:138-144. <http://dx.doi.org/10.1016/j.tsf.2015.12.069>.
- Kumar V, Kumar A, Singh KH S, Kumar P (2011). Broadening of omnidirectional reflection range by cascade 1D photonic crystal. *Optoelectronics Adv. Mater. Rapid Commun.* 5(5):488-490.
- Lee HY, Yao T (2003). Design and evaluation of omnidirectional one dimensional photonic crystals. *J. Appl. Phys.* 93:819-830.
- Lin W, Wang GP, Zhang S (2005). Design and fabrication of omnidirectional reflectors in the visible range. *J. Mod. Opt.* 52:1155-1160.
- Liu X-J, Ma J, Meng X-D, Li H-B, Lu J-B, Li H, Wan-Jin C, Wu X-Y, Zhang S-Q, Wu Y-H (2015). The Quantum Well of One-Dimensional Photonic Crystals. *Adv. Condensed Matter Phys.* <http://dx.doi.org/10.1155/2015/959546>.
- Pandey JP (2017). Enlargement of Omnidirectional Reflection Range Using Cascaded Photonic Crystals. *Int. J. Pure Appl. Phys.* 13(2):167-173.
- Pandey GN, Pandey J P, Mishra AK, Ojha SP (2016). Three dimensional reflectance properties of plasma dielectric photonic crystal. *AIP Conference Proceedings* 1728:020312.
- Pandey GN, Pandey JP, Pandey UK, Sancheti B, Ojha SP (2016). Three dimensional reflectance property of superconductor-dielectric photonic crystal. (ICC 2015) *AIP Conf. Proc.* 1728: 020306.
- Prasad S, Singh V, Singh AK (2011). Effect of inhomogeneous plasma density on the reflectivity in one dimensional plasma photonic crystal. *Prog. Electromagn. Res. M* 21:211.
- Segev M, Soljačić M, Dudley JM (2012). Fractal optics and beyond. *Nature Photonics* 6:209.
- Singh SK, Thapa KB, Ojha SP (2006). Large frequency range of omnidirectional reflection in Si-based one dimensional photonic crystals. *Int. J. Micro. Opt. Technol.* 1(2):686-690.
- Singh SK, Pandey JP, Thapa KB, Ojha SP (2007). Structural parameters in the formation of omnidirectional high reflectors. *PIER* 70:53-78.
- Thapa KB, Singh SK, Ojha SP (2006). Omnidirectional high reflector for infrared wavelength. *Int. J. Infrared Milli. Waves* 27:1557-1568.
- Valligatla S, Chiasera A, Varas S, Bazzanella N, Rao DN, Righini GC, Ferrari M (2012). High quality factor 1-D Er<sup>3+</sup> activated dielectric microcavity fabricated by RF sputtering. *Opt. Express* 20:21214-21222.
- Wang X, Hu X, Li Y, Jia W, Xu C, Liu X, Zi J (2002). Enlargement of omnidirectional total reflection frequency range in one-dimensional photonic crystals by using photonic heterostructures. *Appl. Phys. Lett.* 80:4291-4293.
- Winn JN, Fink Y, Fan S, Joannopoulos JD (1998). Omnidirectional reflection from a one-dimensional photonic crystal. *Opt. Lett.* 23:1573-1575.
- Wu CJ, Chung YH, Syu BJ, Yang TJ (2010). Band gap extension in a one-dimensional ternary metal-dielectric photonic crystal. *PIER* 102:81-93.
- Yeh P (1988). *Optical Waves in Layered Media*. (New York: John Wiley and Sons).
- Zhang HF, Chen YQ (2017). The properties of two-dimensional fractal plasma photonic crystals with Thue-Morse sequence. *Phys. Plasmas* 24:042116.
- Zhang HF, Ma L, Liu SB (2009). Study of periodic band gap structure of the magnetized plasma photonic crystals. *Optoelectronics Lett.* 5:112.
- Zhang HF, Liu SB (2016a). Analyzing the photonic band gaps in two-dimensional plasma photonic crystals with fractal Sierpinski gasket structure based on the Monte Carlo method. *AIP Adv.* 6: 085116.
- Zhang HF, Liu SB (2016b). Enhanced the tunable omnidirectional photonic band gaps in the two-dimensional plasma photonic crystals. *Opt. Quant. Electron.* 48:508.
- Zhang HF, Liu SB, Kong XK (2013a). Investigation of Faraday effects in photonic band gap for tunable three-dimensional magnetized plasma photonic crystals containing the anisotropic material in diamond arrangement. *J. Electromagn. Wave Appl.* 27:1776.
- Zhang HF, Liu SB, Kong XK (2013b). Properties of anisotropic photonic band gaps in three-dimensional plasma photonic crystals containing the uniaxial material with different lattices. *Prog. Electromagn. Res.* 141:267.
- Zhang HF, Liu SB, Kong XK (2013c). Enlarged omnidirectional band gap in one-dimensional plasma photonic crystals with ternary Thue-Morse aperiodic structure. *Physica B.* 410:244.
- Zhang HF, Zhen JP, He WP (2013d). Omnidirectional photonic band gaps enhanced by Fibonacci quasiperiodic one-dimensional ternary plasma photonic crystals. *Optik* 124:4182.